Hindawi Publishing Corporation
Advances in Power Electronics
Volume 2011, Article ID 621818, 8 pages
doi:10.1155/2011/621818

Research Article

Investigation of SSR Characteristics of Hybrid Series Compensated Power System with SSSC

R. Thirumalaivasan,[1] M. Janaki,[1] and Nagesh Prabhu[2]

[1] *School of Electrical Engineering, VIT University, Vellore 632014, India*
[2] *Canara Engineering College, Benjanapadavu, Bantwal, Mangalore 574219, India*

Correspondence should be addressed to R. Thirumalaivasan, thirumalai.r@vit.ac.in

Received 2 November 2010; Accepted 13 March 2011

Academic Editor: Henry S. H. Chung

Copyright © 2011 R. Thirumalaivasan et al. This is an open access article distributed under the Creative Commons Attribution License, which permits unrestricted use, distribution, and reproduction in any medium, provided the original work is properly cited.

The advent of series FACTS controllers, thyristor controlled series capacitor (TCSC) and static synchronous Series Compensator (SSSC) has made it possible not only for the fast control of power flow in a transmission line, but also for the mitigation of subsynchronous resonance (SSR) in the presence of fixed series capacitors. SSSC is an emerging controller and this paper presents SSR characteristics of a series compensated system with SSSC. The study system is adapted from IEEE first benchmark model (FBM). The active series compensation is provided by a three-level twenty four-pulse SSSC. The modeling and control details of a three level voltage source converter-(VSC)-based SSSC are discussed. The SSR characteristics of the combined system with constant reactive voltage control mode in SSSC has been investigated. It is shown that the constant reactive voltage control of SSSC has the effect of reducing the electrical resonance frequency, which detunes the SSR. The analysis of SSR with SSSC is carried out based on frequency domain method, eigenvalue analysis and transient simulation. While the eigenvalue and damping torque analysis are based on linearizing the D-Q model of SSSC, the transient simulation considers both D-Q and detailed three phase nonlinear system model using switching functions.

1. Introduction

Power transfer capability of long transmission line is limited by the transient stability limit. The first swing stability limit of a single machine infinite bus system can be determined through well-known equal-area criterion [1, 2]. During faulted period, the electrical output power of the machine decreases drastically while the input mechanical power remains more or less constant. Thus, the machine acquires excess energy and is used to accelerate the machine. The excess energy during faulted period can be represented by an area called accelerating area. To maintain stability, the machine must return the excess energy once the fault is cleared. The excess energy returning capability of the machine in postfault period is represented by another area called decelerating area. Thus, the stability of the system can be improved by enlarging the decelerating area, and it requires raising the power-angle curve of the system. Flexible AC transmission systems (FACTS) devices are found to be very effective in improving both stability and damping of a power system by dynamically controlling the power-angle curve of the system [1, 2]. With SSSC, working in capacitive mode, net reactance is reduced, and, during the first swing, sufficient decelerating area is introduced to counterbalance the accelerating area. However, in the subsequent swings, the SSSC provides better damping than that of the STATCOM when supplementary modulation controllers are incorporated [3].

The series capacitor compensation for long-distance power transmission line helps in enhancing power transfer and is an economical solution to improve the system stability compared to addition of new lines. A series capacitor compensated line exhibits a resonant minimum in its impedance at a frequency $f_{er} = f_0 = \sqrt{X_C/X_L}$, where X_C is the capacitive compensating reactance, X_L is inductive line reactance, and f_0 is the synchronous frequency of the power system. The resonant frequency f_{er} of the compensated line depends on the level of compensation of the line inductance but is always subsynchronous since, in practice, the compensation ratio is less than unity. It is the coupling of this subsynchronous electrical transmission line resonance to the mechanical resonances of a multistage turbine-generator that gives rise to the phenomenon of SSR. The problem of self-excited torsional frequency oscillations (due to torsional interactions) was experienced at Mohave power station in USA. in December 1970 and October 1971 [3, 4].

The hybrid compensation consisting of suitable combination of passive elements and active FACTS controller such as TCSC or SSSC can be used to mitigate SSR [5]. SSSC is a new generation series FACTS controller based on VSC and has several advantages over TCSC based on thyristor controllers. An ideal SSSC is essentially a pure sinusoidal AC voltage source at the system fundamental frequency. The voltage is always injected in quadrature with the line current, thereby emulating an inductive or a capacitive reactance in series with the transmission line [3]. SSSC output impedance at other frequencies is ideally zero. Thus, SSSC does not resonate with the inductive line impedance to initiate subsynchronous resonance oscillations. However, in hybrid series compensation, fixed capacitor element contributes for series resonance.

The SSSC has only one degree of freedom (i.e, reactive voltage control, unless there is an energy source connected on the DC side of VSC which allow for real power exchange) which is used to control active power flow in the line [3]. The VSC based on three-level converter topology greatly reduces the harmonic distortion on the AC side [3, 6, 7]. In this paper fixed series capacitor and active compensation provided by three-level twenty four-pulse VSC-based SSSC are considered. The constant reactive voltage control of SSSC is considered. The major objective is to investigate SSR characteristics of the series compensated system with SSSC using both linear analysis and nonlinear transient simulation. It is shown that the constant reactive voltage control of SSSC has the effect of reducing the electrical resonance frequency, which detunes SSR.

The study is carried out based on frequency domain method, eigenvalue analysis and transient simulation [8]. The modelling of the system neglecting VSC is detailed (including network transients) and can be expressed in DQ variables or (three) phase variables. The modeling of VSC is based on (1) DQ variables (neglecting harmonics in the output voltages of the converters) and (2) phase variables and the use of switching functions. The damping torque analysis, eigenvalue analysis, and the controller design is based on the DQ model while the transient simulation considers both models of VSC. The results based on linear analysis are validated using transient simulation based on nonlinear system model.

The paper is organized as follows. Section 2 describes the modelling of SSSC whereas the different methods of analysis of SSR are discussed in Section 3. Section 4 describes a case study and investigates the SSR characteristics with SSSC. The major conclusions of the paper are given in Section 5.

2. Modelling of SSSC with Three-Level VSC

Figure 1 shows the schematic representation of SSSC. In the power circuit of an SSSC, the converter is usually either a multipulse or a multilevel configuration. The elimination of voltage harmonics requires multi-pulse configuration of VSC. The multi-pulse converters are generally of TYPE-2 where only the phase angle of converter output voltage can be controlled and modulation index of the converter remains fixed [3].

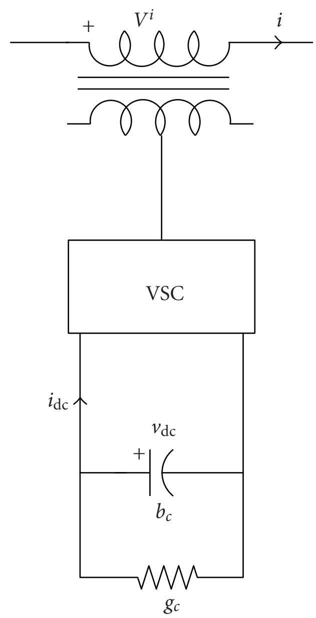

Figure 1: Schematic representation of SSSC.

When the DC voltage is constant, the magnitude of ac output voltage of the converter can be changed by Pulse Width Modulation (PWM) with two-level topology which demands higher switching frequency and leads to increased losses. In three level converter topology, both the magnitude and phase angle of converter output voltage can be controlled. This converter is classified as TYPE-1 converter [9], where DC bus voltage is maintained constant and the magnitude of converter output voltage is controlled by varying dead angle β with fundamental switching frequency modulation [3, 10]. The harmonics are dependent on the capacitance and the operating point of the SSSC. The detailed three-phase model of SSSC is developed by modelling the converter operation by switching functions. The switching function for phase "a" is shown in Figure 2.

The switching functions of phases b and c are similar but phase shifted successively by 120° in terms of the fundamental frequency. Assuming that the dc capacitor voltages $V_{dc1} = V_{dc2} = V_{dc}/2$, the converter terminal voltages with respect to the midpoint of dc side "N" can be obtained as

$$\begin{bmatrix} V_{aN}^i \\ V_{bN}^i \\ V_{cN}^i \end{bmatrix} = \begin{bmatrix} P_a(t) \\ P_b(t) \\ P_c(t) \end{bmatrix} \frac{V_{dc}}{2}, \tag{1}$$

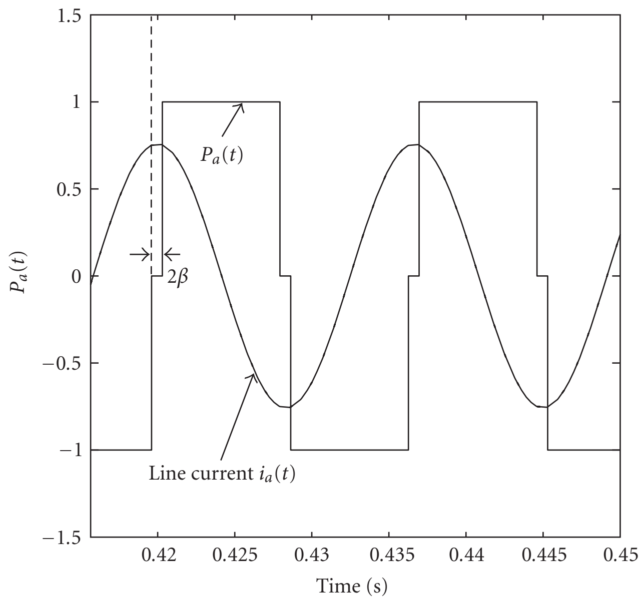

Figure 2: Switching function for a three level converter.

and the converter output voltages with respect to the neutral of transformer can be expressed as

$$\begin{bmatrix} V_{an}^i \\ V_{bn}^i \\ V_{cn}^i \end{bmatrix} = \begin{bmatrix} S_a(t) \\ S_b(t) \\ S_c(t) \end{bmatrix} V_{\text{dc}}\ , \tag{2}$$

where

$$S_a(t) = \frac{P_a(t)}{2} - \left[\frac{P_a(t) + P_b(t) + P_c(t)}{6}\right]. \tag{3}$$

$S_a(t)$ is the switching function for phase "a" of a 6-pulse 3-level VSC. Similarly for phase "b", $S_b(t)$, and for phase "c", $S_c(t)$ can be derived. The peak value of the fundamental and harmonics in the phase voltage V_{an}^i are found by applying Fourier analysis on the phase voltage and can be expressed as

$$V_{an(h)}^i = \frac{2}{h\pi} V_{\text{dc}} \cos(h\beta), \tag{4}$$

where, $h = 1, 5, 7, 11, 13$, and β is the dead angle (period) during which the converter pole output voltage is zero. We can eliminate the 5th and 7th harmonics by using a twelve-pulse VSC, which combines the output of two six-pulse converters using transformers.

The switching functions for first twelve-pulse converter are given by

$$\begin{aligned} S_{1a}^{12}(t) &= S_{1a}(t) + \frac{1}{\sqrt{3}}\left(S'_{1a}(t) - S'_{1c}(t)\right), \\ S_{1b}^{12}(t) &= S_{1b}(t) + \frac{1}{\sqrt{3}}\left(S'_{1b}(t) - S'_{1a}(t)\right), \\ S_{1c}^{12}(t) &= S_{1c}(t) + \frac{1}{\sqrt{3}}\left(S'_{1c}(t) - S'_{1b}(t)\right), \end{aligned} \tag{5}$$

where

$$\begin{aligned} S'_{1x}(t) &= S_{1x}\left[t + \frac{2\pi}{\omega_o}\frac{1}{12}\right] \\ S_{1x}(t) &= S_x\left[t + \frac{\pi}{\omega_o}\frac{1}{24}\right], \quad x = a, b, c. \end{aligned} \tag{6}$$

The switching functions for second twelve-pulse converter are given by

$$\begin{aligned} S_{2a}^{12}(t) &= S_{2a}(t) + \frac{1}{\sqrt{3}}\left(S'_{2a}(t) - S'_{2c}(t)\right), \\ S_{2b}^{12}(t) &= S_{2b}(t) + \frac{1}{\sqrt{3}}\left(S'_{2b}(t) - S'_{2a}(t)\right), \\ S_{2c}^{12}(t) &= S_{2c}(t) + \frac{1}{\sqrt{3}}\left(S'_{2c}(t) - S'_{2b}(t)\right), \end{aligned} \tag{7}$$

where

$$\begin{aligned} S'_{2x}(t) &= S_{2x}\left[t + \frac{2\pi}{\omega_o}\frac{1}{12}\right] \\ S_{2x}(t) &= S_x\left[t - \frac{\pi}{\omega_o}\frac{1}{24}\right], \quad x = a, b, c. \end{aligned} \tag{8}$$

The switching functions for a twenty four-pulse converter are given by

$$S_x^{24}(t) = S_{1x}^{12}(t) + S_{2x}^{12}(t), \quad x = a, b, \text{ and } c. \tag{9}$$

If the switching functions are approximated by their fundamental components (neglecting harmonics) for a 24-pulse three level converter, we get

$$V_{\text{an}}^i = \frac{8}{\pi} V_{\text{dc}} \cos(\beta) \sin(\omega_o t + \phi + \gamma), \tag{10}$$

and V_{bn}^i, V_{cn}^i are phase shifted successively by 120°.

The line current is given by $i_a = \sqrt{2/3} I_a \sin(\omega_o + \phi)$ and i_b, i_c are phase shifted successively by 120°. Note that γ is the angle by which the fundamental component of converter output voltage leads the line current. It should be noted that γ is nearly equal to $\pm\pi/2$ depending on whether SSSC injects inductive or capacitive voltage. Neglecting converter losses, we can get the expression for dc capacitor current as

$$\left[i_{\text{dc}}\right] = -\left[S_a^{24}(t) \ \ S_b^{24}(t) \ \ S_c^{24}(t)\right] \begin{bmatrix} i_a \\ i_b \\ i_c \end{bmatrix}. \tag{11}$$

A particular harmonic reaches zero when $2\beta = 180°/h$. At $\beta_{\text{optimum}} = 3.75°$, the three level 24-pulse converter behaves nearly like a two-level 48-pulse converter as 23th and 25th harmonics are negligibly small.

2.1. Modelling of SSSC in D-Q *Variables.* When switching functions are approximated by their fundamental frequency components, neglecting harmonics, SSSC can be modelled by transforming the three-phase voltages and currents to D-Q variables using Kron's transformation [2]. The SSSC can be represented functionally as shown in Figure 3.

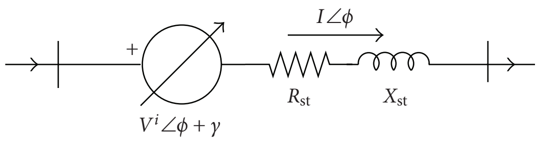

FIGURE 3: Equivalent circuit of SSSC as viewed from AC side.

In Figure 3, R_{st} and X_{st} are the resistance and reactance of the interfacing transformer of VSC. The magnitude control of converter output voltage V^i is achieved by modulating the conduction period affected by dead angle of converter while dc voltage is maintained constant.

The converter output voltage can be represented in D-Q frame of reference as

$$V^i = \sqrt{V_D^{i\,2} + V_Q^{i\,2}},$$
$$V_D^i = k_m V_{dc} \sin(\phi + \gamma), \quad (12)$$
$$V_Q^i = k_m V_{dc} \cos(\phi + \gamma),$$

where $k_m = k\rho \cos\beta_{se}$; $k = 4\sqrt{6}/\pi$ for a 24-pulse converter. ρ is the transformation ratio of the interfacing transformer.

From a control point of view, it is convenient to define the active voltage ($V_{P(se)}$) and reactive ($V_{R(se)}$) voltage injected by SSSC in terms of variables in D-Q frame (V_D^i and V_Q^i) as follows

$$V_{R(se)} = V_D^i \cos\phi - V_Q^i \sin\phi,$$
$$V_{P(se)} = V_D^i \sin\phi + V_Q^i \cos\phi. \quad (13)$$

Here, positive $V_{R(se)}$ implies that SSSC injects inductive voltage and positive $V_{P(se)}$ implies that it draws real power to meet losses.

The dc side capacitor is described by the dynamical equation as

$$\frac{dV_{dc}}{dt} = -\frac{g_c\omega_b}{bc}V_{dc} - i_{dc}\frac{\omega_b}{bc}, \quad (14)$$

where $i_{dc} = -[k_m \sin(\phi+\gamma)I_D + k_m \cos(\phi+\gamma)I_Q]$, I_D and I_Q are the D-Q components of the line current.

2.2. Type-1 Controller. In this type of controller, both magnitude (modulation index k_m) and phase angle of converter output voltage (γ) are controlled. The capacitor voltage is maintained at a constant voltage by controlling the active component of the injected voltage $V_{P(se)}$. The real voltage reference $V_{P(se)(ord)}$ is obtained as the output of DC voltage controller. The reactive voltage reference $V_{R(se)(ord)}$ may be kept constant or obtained from a power scheduling controller. However, for the SSR analysis, constant reactive voltage control is considered.

It should be noted that harmonic content of the SSSC-injected voltage would vary depending upon the operating point since magnitude control will also govern the switching. The capacitor voltage reference can be varied (depending on reactive voltage reference) so as to give optimum harmonic performance. In three level 24-pulse converter, dc voltage reference may be adjusted by a slow controller to get optimum harmonic performance at $\beta_{se} = 3.75°$ in steady state.

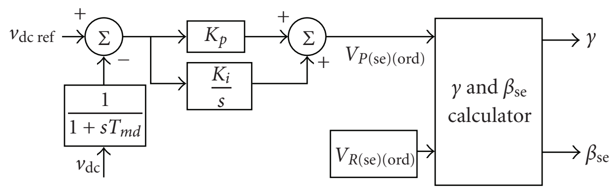

FIGURE 4: Type-1 controller for SSSC.

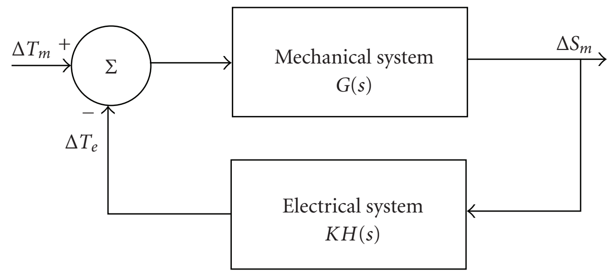

FIGURE 5: Interaction between mechanical and electrical system.

The structure of type-1 controller for SSSC is given in Figure 4. In Figure 4, γ and β_{se} are calculated as

$$\gamma = \tan^{-1}\left[\frac{V_{R(se)(ord)}}{V_{P(se)(ord)}}\right],$$
$$\beta_{se} = \cos^{-1}\left[\frac{\sqrt{V_{P(se)(ord)}^2 + V_{R(se)(ord)}^2}}{k_m V_{dc}}\right]. \quad (15)$$

3. Analysis of SSR

The two aspects of SSR are [4](i) steady-state SSR (induction generator effect (IGE) and torsional interaction (TI)) (ii) shaft torque amplification due to transients. The analysis of steady-state SSR can be done by linearized models at the operating point and include damping torque analysis and eigenvalue analysis. The analysis of shaft torque amplification due to transients requires transient simulation of the nonlinear model of the system. For the analysis of SSR, it is adequate to model the transmission line by lumped resistance and inductance where the line transients are also considered. The generator stator transients are also considered by using detailed (2.2) model of the generator.

The analysis of SSR is carried out based on damping torque analysis, eigenvalue analysis, and transient simulation.

3.1. Damping Torque Analysis. Damping torque analysis is a frequency domain method which can be used to screen the system conditions that give rise to potential SSR problems involving torsional interactions. It also enables the planners to decide on a suitable countermeasure for the mitigation of the detrimental effects of SSR. Damping torque method gives

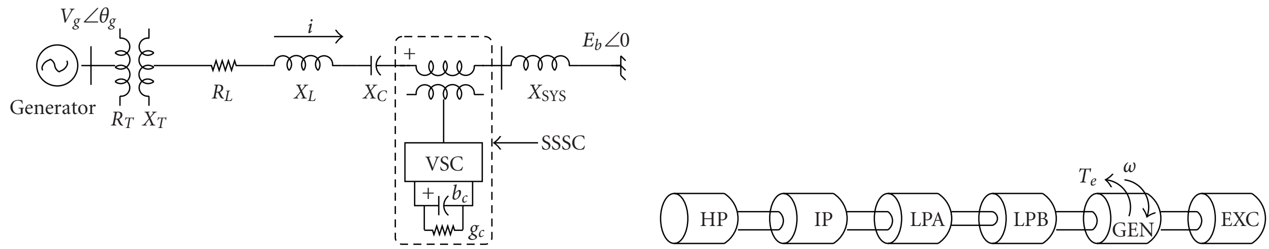

(a) Electrical System (b) Six mass mechanical system

Figure 6: Modified IEEE first benchmark model with SSSC.

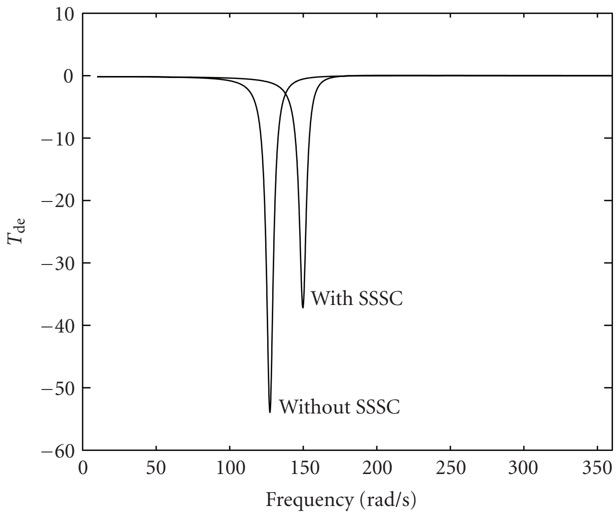

Figure 7: Damping torque with admittance function in D-Q axes.

a quick check to determine the torsional mode stability. The system is assumed to be stable if the net damping (including electrical and mechanical) at any of the torsional mode frequency is positive.

The interaction between the electrical and mechanical system can be represented by the block diagram shown in Figure 5. (ΔS_m) is the p.u. deviation in generator rotor speed, and (ΔT_e) is the p.u. change in electric torque [11].

The transfer function relating (ΔT_e) to (ΔS_m) is $KH(s)$. At any given oscillation frequency of the generator rotor, the component of electrical torque (ΔT_e) in phase with the rotor speed (ΔS_m) is termed as damping torque. The damping torque coefficient ($T_{de}(\omega)$) is defined as follows:

$$T_{de}(\omega) = \Re\left[\frac{\Delta T_e(j\omega)}{\Delta S_m(j\omega)}\right] = \Re[H(j\omega)]_{K=1}. \quad (16)$$

In obtaining (16), it is necessary to express the impedance function $[Z_s]$ of SSSC in D-Q frame [8].

3.2. Eigenvalue Analysis. In this analysis, the detailed generator model (2.2) [2] is considered. The electromechanical system consists of the multimass mechanical system, the generator, the excitation system, power system stabilizer (PSS), torsional filter, and the transmission line with SSSC. The SSSC equations (12)–(14) along with the equations representing electromechanical system [2, 4] (in D-Q variables), are linearized at the operating point, and eigenvalues of system matrix are computed. The stability of the system is determined by the location of the eigenvalues of system matrix. The system is stable if the eigenvalues have negative real parts.

3.3. Transient Simulation. The eigenvalue analysis uses equations in D-Q variables neglecting the harmonics. To validate the results obtained from damping torque and eigenvalue analysis, the transient simulation should be carried out using detailed nonlinear three-phase model of SSSC which considers the switching in the thyristors/three-phase converters. The actual converter switching of the SSSC based on three level 24-pulse converter is modelled by generating switching functions.

4. A Case Study

The system considered is a modified IEEE FBM [12]. The complete electromechanical system is represented schematically in Figure 6, which consists of a generator, turbine, and series compensated long transmission line with SSSC injecting a reactive voltage in series with the line. The electrical system data is taken from [8].

The modelling aspects of the electromechanical system comprising the generator, and the mass-spring mechanical system, the excitation system, power system stabilizer (PSS) with torsional filter, and the transmission line containing the conventional series capacitor are discussed in [4]. The analysis is carried out on the IEEE FBM based on the following initial operating condition and assumptions.

(1) The generator delivers 0.9 p.u. power to the transmission system.

(2) The input mechanical power to the turbine is assumed constant.

(3) The total series compensation level is set at 0.6 p.u.

(4) For transient simulation, a step decrease of 10% mechanical input torque applied at 0.5 sec and removed at 1 sec is considered in all case studies.

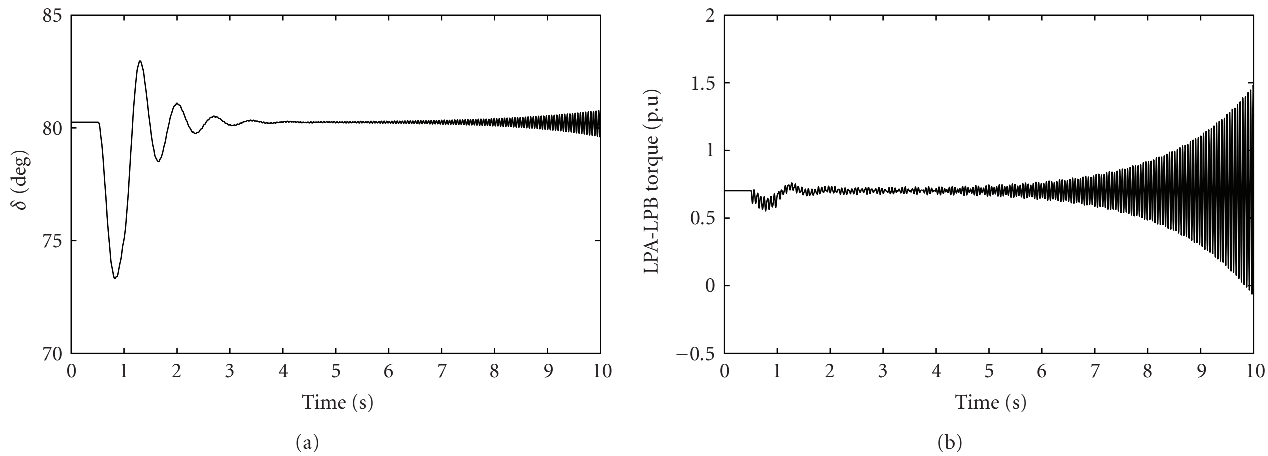

Figure 8: System response without SSSC.

4.1. Damping Torque Analysis. The damping torque due to electrical network is evaluated in the range of frequency of 10–360 rad/sec for the following cases using (14).

(1) Without SSSC,

(2) With SSSC.

In case (1), the series compensation of 60% is completely met by fixed capacitor and in case (2), hybrid compensation is used wherein 45% of compensation is met by fixed capacitor and the remaining 15% by SSSC. The variation of damping torque with frequency for both cases is shown in Figure 7.

It is to be noted that, in case (1), the damping torque is maximum negative at a frequency of around 127 rad/sec which matches with the natural frequency of torsional mode-2 and adverse torsional interactions are expected. In case (2), maximum undamping occurs at a frequency of about 150 rad/sec. Since this network frequency mode is not coinciding with any of the torsional modes, the system is stable.

4.2. Eigenvalue Analysis. In this analysis, generator model (2.2) is considered. The SSSC equations along with the equations representing electromechanical system considering mechanical damping are linearized at the operating point. The eigenvalues of system matrix are computed and are given in Table 1. It is to be noted that inclusion of SSSC leads to a stable system and reduces the potential risk of SSR problem.

Table 1: Eigen values of the combined system.

Torsional mode	Eigenvalue	
	Without SSSC	With SSSC
0	$-1.7366 \pm j$ 8.9279	$-1.2987 \pm j\,8.1094$
1	$-0.2143 \pm j\,99.4580$	$-0.2132 \pm j\,99.135$
2	$0.6658 \pm j\,127.000$	$-0.0695 \pm j\,127.050$
3	$-0.6459 \pm j\,160.420$	$-0.6438 \pm j\,160.210$
4	$-0.3646 \pm j\,202.820$	$-0.3694 \pm j\,202.800$
5	$-1.8504 \pm j\,298.170$	$-1.8504 \pm j\,298.170$
Network mode	$-1.9029 \pm j\,126.950$	$-1.4918 \pm j\,149.980$
Network mode	$-2.9906 \pm j\,626.790$	$-2.4803 \pm j\,582.980$

4.3. Transient Simulation. The eigenvalue analysis uses equations in D-Q variables where the switching functions are approximated by their fundamental components (converter switchings are neglected). To validate the results obtained from damping torque and eigenvalue analysis, the transient simulation should be carried out using detailed model of SSSC which considers the switching of three-phase converter. Hence, the three level 24-pulse converter is modelled by generating switching functions. The transient simulation of the combined system with detailed three-phase model of SSSC has been carried out using MATLAB-SIMULINK [13]. The system response for simulation without SSSC is shown in Figure 8. The simulation results of combined system with detailed three phase model of SSSC is shown in Figure 9. It is to be noted that the system is stable with the inclusion of SSSC for the constant reactive voltage control.

4.4. Discussion. The representation of impedance function of SSSC in single-phase basis ($Z_{s(1\text{ph})}(j\omega)$) from that of D-Q axes $[Z_s]$ [8] is approximate and is given below

$$Z_{s(1\text{ph})} = \frac{1}{2}\left[\left\{Z_{s\text{DD}}(j(\omega-\omega_0)) + Z_{s\text{QQ}}(j(\omega-\omega_0))\right\} + j\left\{Z_{s\text{DQ}}(j(\omega-\omega_0)) - Z_{s\text{QD}}(j(\omega-\omega_0))\right\}\right]. \quad (17)$$

The resistance R_{se} and reactance X_{se} of SSSC on single phase basis as a function of frequency ω_{er} are computed for $X_{\text{sssc}} = 0.15$ with constant reactive voltage control. It is found that the resistance is negligible while the reactance X_{se} is practically constant with frequency.

The effect of inclusion of SSSC on the resonance frequency is shown in Figure 10 for cases 1 and 2.

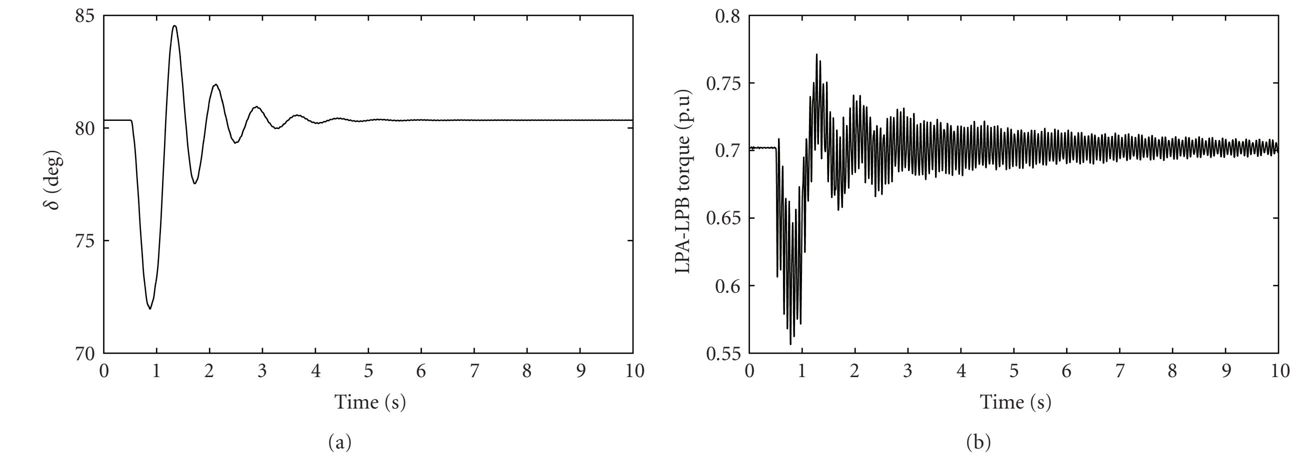

Figure 9: System response with detailed three phase model of SSSC.

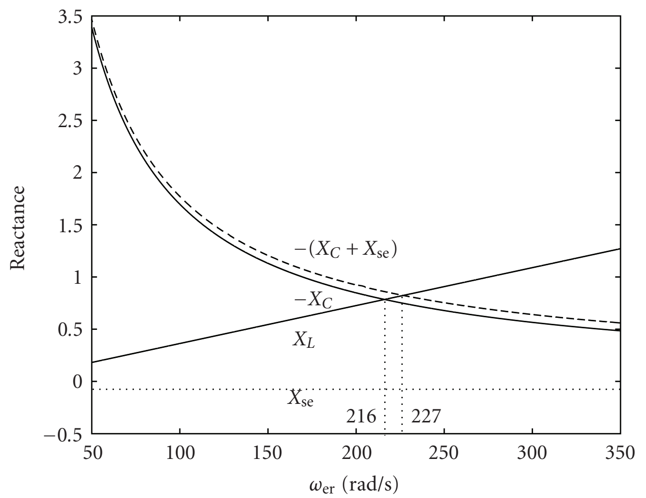

Figure 10: Graphical representation of resonance conditions with and without SSSC.

When the fixed capacitor provides 45% compensation, the resonance occurs at $\omega_{\text{er}} = 216$ rad/sec where $X_C = X_L$. When the additional compensation of 15% is provided by SSSC, the effective capacitive reactance $(X_C + X_{\text{se}})$ is obtained by adding the constant reactance offered by SSSC to that offered by fixed capacitor. The variation of effective capacitive reactance $(X_C + X_{\text{se}})$ with frequency is also shown in Figure 10. Now, the resonance occurs at a higher frequency of $\omega_{\text{er}} = 227$ rad/sec where $(X_C + X_{\text{se}}) = X_L$ and this is consistent with the subsynchronous network mode frequency (ω_0-ω_{er} = 377-227 = 150) of about 150 rad/sec as obtained with damping torque analysis with SSSC.

The effect of providing additional series compensation by SSSC to supplement the existing fixed capacitor is to increase the electrical resonance frequency of the network. However, this increase in frequency is not significant as compared to that obtained with the equivalent fixed capacitor offering additional compensation (case 1) $\omega_{\text{er}} = 250$ rad/sec in this case. This indicates that the SSSC is not strictly SSR neutral however, it offers a reactance which remains practically constant with frequency.

5. Conclusion

In this paper, we have presented the analysis and simulation of a hybrid series compensated system with SSSC. The modelling details of 24-pulse three level VSC-based SSSC is presented. The application of D-Q model is validated by the transient simulation of the three-phase model of SSSC.

There is no appreciable difference in the resonance frequency of the electrical network as the total series compensation (in a hybrid compensation scheme) is increased by increasing the series reactive voltage injected, instead of the series capacitor. This reduces the risk of SSR as the fixed capacitor can be chosen such that the electrical resonance frequency does not coincide with the complement of the torsional modal frequency (which is practically independent of the electrical network). It is observed that the injected reactive voltage can be adjusted to detune the SSR. The case studies indicated that the SSSC is not strictly SSR neutral however, it offers a reactance which remains practically constant with frequency.

References

[1] N. G. Hingorani and L. Gyugyi, *Understanding FACTS*, IEEE Press, New York, NY, USA, 2000.

[2] K. R. Padiyar, *Power System Dynamics—Stability and Control*, B.S.Publications, Hyderabad, India, 2nd edition, 2002.

[3] K. R. Padiyar, *FACTS Controllers in Power Transmission and Distribution*, New Age International (P) Limited, New Delhi, India, 2007.

[4] K. R. Padiyar, *Analysis of Subsynchronous Resonance in Power Systems*, Kluwer Academic Publishers, Boston, Mass, USA, 1999.

[5] K. R. Padiyar and N. Prabhu, "Analysis of SSR with three-level twelve-pulse VSC-based interline power-flow controller," *IEEE Transactions on Power Delivery*, vol. 22, no. 3, pp. 1688–1695, 2007.

[6] R. W. Menzis and Y. Zhuang, "Advanced static compensationusing a multilevel GTO thyristor inverter," *IEEE Transactions on PowerDelivery*, vol. 10, no. 2, 1995.

[7] J. B. Ekanayake and N. Jenkins, "Mathematical models of a three-level advanced static VAr compensator," *IEE Proceedings*, vol. 144, no. 2, pp. 201–206.

[8] K. R. Padiyar and N. Prabhu, "Analysis of subsynchronous resonance with three level twelve-pulse VSC based SSSC," in *Proceedings of the IEEE Confernce on Covergent Technologies for the Asia-Pacific Region (TENCON '03)*, pp. 76–80, October 2003.

[9] C. Schauder and H. Mehta, "Vector analysis and control of advanced static VAR compensators," *IEE Proceedings C*, vol. 140, no. 4, pp. 299–306, 1993.

[10] K. K. Sen and E. J. Stacey, "UPFC—Unified Power Flow Controller: theory, modeling, and applications," *IEEE Transactions on Power Delivery*, vol. 13, no. 4, pp. 1453–1460, 1998.

[11] N. Prabhu and K. R. Padiyar, "Investigation of subsynchronous resonance with VSC-based HVDC transmission systems," *IEEE Transactions on Power Delivery*, vol. 24, no. 1, pp. 433–440, 2009.

[12] IEEE Subsynchronous Resonance Task Force, "First bench mark model for computer simulation of Subsynchronous resonance," *IEEE Transactions on Power Apparatus and Systems*, vol. 96, no. 5, pp. 1565–1572, 1977.

[13] The Math works Inc, "Using MATLAB-SIMULINK," 1999.


Journal of Engineering
The Scientific World Journal
International Journal of Rotating Machinery
Journal of Sensors
International Journal of Distributed Sensor Networks
Advances in Civil Engineering
Hindawi
Submit your manuscripts at
http://www.hindawi.com
Journal of Control Science and Engineering
Journal of Robotics
Journal of Electrical and Computer Engineering
Advances in OptoElectronics
VLSI Design
International Journal of Navigation and Observation
Modelling & Simulation in Engineering
International Journal of Aerospace Engineering
International Journal of Chemical Engineering
International Journal of Antennas and Propagation
Active and Passive Electronic Components
Shock and Vibration
Advances in Acoustics and Vibration